Fourier resolved spectroscopy of 4U 1728–34: New Insights into Spectral and Temporal Properties of Low-Mass X-ray Binaries

C.R. Shrader[1,4], P. Reig[2,3] and D. Kazanas[1]

[1] Astrophysics Science Division, NASA Goddard Space Flight Center, Greenbelt, MD 20771
[2]IESL, Foundation for Research and Technology, 711 10 Heraklion, Crete, Greece
[3]Physics Department, University of Crete, PO Box 2208, 710 03 Heraklion, Crete, Greece
[4] University Space Reseach Association, 10211 Wincopin Circle, Suite 620, Columbia, MD 21044

Chris.R.Shrader@gsfc.nasa.gov, pau@physics.uoc.gr, Demos.Kazanas-1@nasa.gov

Received —————————; accepted —————————

ABSTRACT

Using archival RXTE data we derive the 2-16 keV Fourier-resolved spectra of the Atoll source 4U 1728–34 in a sequence of its timing states as its low QPO frequency spans the range between 6 and 94 Hz. The increase in the QPO frequency accompanies a spectral transition of the source from its island to its banana states. The banana-states' Fourier-resolved spectra are well fitted by a single blackbody component with $kT \sim 2 - 3$ keV depending on the source position in the color – color diagram and the Fourier frequency, thus indicating that this spectral component is responsible for the source variability on these timescales. This result is in approximate agreement with similar behavior exhibited by the Z sources, suggesting that, as in that case, the bounday layer – the likely source of the thermal component – is supported by radiation pressure. Furthermore, it is found that the iron line at ∼6.6 keV, clearly present in the averaged spectra, not apparent within the limitations of our measurements in the frequency-resolved spectra irrespective of the frequency range. This would indicate that this spectral component exhibits little variability on time scales comprising the interval $10^{-2} - 10^2$ seconds. In the island state the single blackbody model proved inadequate, particularly notable in our lowest frequency band $(0.008 - 0.8$ Hz). An absorbed powerlaw or an additive blackbody plus hard powerlaw model was required to obtain a satisfactory fit. Statisics do not allow unambiguous discrimination between these possible scenarios.

Subject headings: accretion, accretion disks — neutron stars — stars: individual (4U 1728–34) — X-rays: stars

1. Introduction

Rapid X-ray variability and spectral distributions are powerful probes of the physics of accretion flows onto compact objects, i.e. onto neutron stars and black holes. More than two decades of persistent efforts to probe and comprehend the physics involved in these flows led to the accumulation of a wealth of data of both their spectra and time variations. Significant progress in both these directions has been made over the last decade, in particular, with the wealth of data provided by the Rossi X-Ray Timing Explorer (RXTE). Its large collecting area and high time resolution have facilitated detailed studies on the rapid variability and the spectra of a large sample of sources. However, the accompanying improvement in the understanding of the dynamics and radiation emission physics associated with these accretion powered sources has progressed considerably slower than the accumulation of the data and their ensuing classification within semi-coherent phenomenological models.

Concerning the differentiation between the spectral and timing characteristics of accreting neutron stars and black holes, the former appeared to present higher complexity in both their spectral and timing properties than the latter. This additional complexity is generally attributed to the presence of the neutron star surface which can complicate the dynamics of accretion and as a result the ensuing spectral and timing properties. In the temporal domain, the power density spectra (PDS) of neutron star low-mass X-ray binaries (LMXBs) exhibit a variety of features ranging from narrow quasi-periodic oscillations (QPOs) to broad noise components (for a review, see Wijnands (2001); also van der Klis (2006) and references therein), only some of which appear to have corresponding features in the black hole case. In the spectral domain, while Comptonization is presumably the predominant process for producing the observed X-ray emission above ~ 1 keV, the neutron-star LMXB spectra are quite complex, more so than those of accreting black hole candidates. This is likely due to the fact that a number of components contribute to the emission in this energy range and that their individual spectra are hard to disentangle.

A simplified way to classify the (apparently complex) spectra of these sources has been that of the color-color (or color - intensity) diagrams (Hasinger & van der Klis 1989); these exhibit, instead of a detailed spectral decomposition, the ratios of fluxes in adjacent bands (colors) within the detector's range (color - color diagrams) or one color as a function of the total flux of the source (color - intensity diagrams). The large body of accumulated data then made it clear that in response to changes in luminosity, these sources cover a certain trajectory in this color - color (or color - intensity) space whose shape has since been used to classify them: The most luminous LMXBs, $L_x \sim 10^{38}$ erg s^{-1}, cover a Z-shape track in color - color space, hence the name Z-sources. The less luminous sources, $L_x \sim 10^{37}$ erg s^{-1}, tend to cover a circular-like path in same space, leading to their designation as atoll sources. At the same time, it was found that there exists a correspondence between their spectral and timing properties, with the frequencies of timing features, such as QPOs or

breaks, generally increasing in response to increases in the X-ray flux and presumably the accretion rate.

The physics governing the spectral and timing properties of Z or atoll sources and their differences remains obscure, although as early as 1984, Mitsuda et al. (1984) noticed the possible decomposition of their spectra into hard and soft components with the hard one being the more variable of the two. A great advance in the understanding of these spectra was made recently with a refinement of the arguments put forward by Mistuda et al. (1984). This involves the implementation of a novel technique that combines the spectral and timing properties of these sources in an effort to produce a coherent picture of the dynamics of these sources.

This technique is known as Fourier Resolved Spectroscopy (FRS) (e.g. Revnivtsev et al. 1999; Zycki 2003; Papadakis et al. 2005, 2006). In short, instead of producing the power spectra as a function of photon energy, as it is customary, this technique accumulates the variability amplitudes over several well defined frequency bands for each energy bin to produce the energy spectra of a source for the specific frequency bands considered. This particular method of presenting the data facilitates the identification of the variable spectral components as well as the time scales over which the variability occurs; as such, it allows certain immediate insights into the dynamics responsible for the emission of the specific spectral components. It was pointed out that this method is particularly suited for the study of spectral features that result from X-ray reprocessing where the light crossing time provides a natural frequency filter; in this case FRS can provide straightforward insights about the geometry of the reprocessing medium. So far, this technique has been applied successfully to galactic black hole candidates (Revnivtsev et al. 1999; Gilfanov et al. 2001; Sobolewska & Zycki 2006; Reig et al. 2006), to neutron-star LMXBs (Gilfanov & Revnivtsev et al 2005) and also to AGN (Papadakis et al. 2005, 2006) yielding insights into variability of different spectral components and infer their spatial arrangements.

Recently, the same technique has been applied to the spectro - temporal data of accreting neutron stars and more specifically to those of Z-sources (Gilfanov et al. 2003; Revnivtsev & Gilfanov 2006). This analysis did confirm the earlier tentative decomposition of the Z-source spectra into a variable hard component and a soft less variable one. The normalization of these components varies with the accretion rate as do their spectra to produce the well known color-color diagram of the Z-sources. In particular, the softer of the two components was identified with the accretion disk and the harder one with the boundary layer of these sources. The temperature of the former was found to change slowly in response changes in luminosity, as expected. The temperature of the boundary layer component remained constant, independent of luminosity and of Fourier frequency. This supports the conjecture that the boundary layer is dominated by radiation pressure. It was also found (Revnivtsev & Gilfanov 2006) that the disk component contributes to the spectra only at the lowest Fourier frequencies. This is consistent with the findings of Reig et al.

(2006) pertaining to the lack of variability of the disk component around a transient black hole LMXB 4U 1543-47. This separation and the identification of these two components in the spectra was possible only because of the combined spectral - timing analysis.

In the present paper we extend the application of the method of Fourier Resolved Spectroscopy to the spectra of a source of the atoll class (i.e. neutron stars accreting at rates ~ 10 times lower than those of Z-sources). The trajectories of these sources in the color-color diagram have a different shape from those of the Z-sources as discussed above. They are known to produce a sequence of states of increasing luminosity known as island, lower banana and upper banana states. Variations in the spectral properties between these states are accompanied by corresponding changes in their timing properties (van der Klis 2006). The source under study is 4U 1728–34, a neutron star LMXB system that is considered to be one of the proto-typical examples of an atoll source. It exhibits variability on a variety timescales, from months down to milliseconds (e.g. Di Salvo et al 2001) as well as exhibiting Type-I bursting behavior.

In §2 we outline the details of our data selection and reduction procedures, while in §3 we describe the FRS methodology. In §4 we present our results for 4U 1728–34 offering our interpretation of the variability of individual spectral components. In §5 we present our general conclusions, including insights gained into accreion geometry and overall physical system configuratons associated with the separate states.

2.   Observations and Data Reduction

Data obtained with RXTE can be collected and telemetered to the ground in many different ways depending on the intensity of a source and the spectral and timing resolution desired. The specific observational modes are selected by the observer and may change during the overall observation. This project requires a temporal sampling of at least twice the highest frequency band to be probed, and enough spectral resolution to separate out the different continuum components as well as to crudely study possible iron line signatures. Since this is an archival study, we had to examine the various datasets for the epochs of interest in order to identify suitable data acquistion modes. Typically, we found that the event-by-event data sampled at 125 microseconds over 64 onboard spectral channels covering the full bandpass of the PCA, suited our purposes. Practically, in order to ensure homogeneity in the reduction process and for signal-to-noise considerations the energy resolution was restricted to be between 16–24 channels covering the energy band 2-16 keV.

Light curves were extracted for each onboard channel range using the current RXTE

software[1], binned at a resolution of 0.0078125 s. We then divided the data into 256-s segments and, following the prescription of Reig et al (2006), we obtained the Fourier resolved spectra of the source in the following broad frequency bands: 0.008-0.8 Hz, 0.8-8 Hz and 8-64 Hz. In total, we examined a total of approximately 54.3 ks of data from the RXTE archives at 7 epochs (see Table 1).

2.1. Spectral Index – QPO Frequency Correlation

It is well established that in accreting neutron star systems, the X-ray luminosity and their spectral and/or timing quantities (X-ray colors, QPO frequencies) tend to correlate with the spectral state of a an individual source, but that these correlations are not identical for the ensemble of sources (see e.g. van der Klis 2006). Furthermore, for a given source, the correlations are much more pronounced over short (hours to days) than on longer time scales (van der Klis 2000 and references therein). Therefore, the use of hardness ratios and source intensity as tracers of the source spectral state can become blurred. In addition, the problem of gain changes associated with the aging of the PCU detectors aboard $RXTE$ makes even the determination and comparison of X-ray colors at different epochs difficult.

To avoid these difficulties we have opted to use one of the QPO frequencies as a proxy for the state of the source. As has been previously pointed out, e.g. van der Klis (2006), the frequencies of all PDS features, most notably QPOs, correlate with the source intensity and also with its spectral state. Furthermore, there is a noted correspondence in the sequence of the spectral and timing states with source intensity between accreting neutron stars and black hole systems.

Motivated by the correlation between the (low-frequency) QPO centroid frequency and photon index in several black-hole XRBs (Vignarca et al. 2003), we have opted to use the corresponding QPO frequency of 4U 1728–34 as a tracer of the configuration changes in the accretion flow. Although as noted above, the neutron star spectra are more complicated than those of the black holes, we find that the correlation between the spectral and timing properties of 4U 1728–34 and similar systems (van der Klis 2006) is sufficiently robust to allow the use of the QPO frequency as an indicator of the spectral state. In fact, Titarchuk & Shaposhnikov (2005) found a correlation between the QPO frequency and their spectral index parameter Γ in their analysis of 4U 1728–34. However, given that its spectrum is more complicated than those of galactic black holes one should not consider this correlation to be universal.

---

[1]http://heasarc.gsfc.nasa.gov/docs/software/lheasoft/

3. Conventional Spectral and Timing Analysis

Fig 1 shows typical energy spectra of the source corresponding to the observational periods selected. The spectra were extracted from PCA *Standard 2* mode data, and in this case no Fourier frequency decomposition has been applied. The response matrix and background models were created using the standard HEADAS software, version 5.3. The number of detectors (PCU) that were switched on for each observation varies, and, in order to be able to compare the spectra, we divided them by the respective number of PCUs.

The spectral analysis was performed using the XSPEC analysis package version 11.3.1. We have added systematic errors of 1% to all channels and have restricted our analysis to the 2-16 keV band only (to match the energy band used in the case of the Fourier-resolved spectra). The results are listed in Table 2. The errors quoted for the best fit values correspond to the 90% confidence limit for one interesting parameter.

We analyzed data at seven different epochs as indicated in Table 1. The 21 and 26 September 1997, 25 January 1999 and 9 February 2001, observations were selected because they span a wide range in both the QPO and break frequencies, ν_1 and ν_b, respectively, as well as the spectral parameter Γ of (Titarchuk & Shaposhnikov 2005). As mentioned above we inferred the spectral state of 4U 1728–34 for a given observation based on the pair (Γ, ν_b). In three cases, 7 June 2001, 18 February 1996, and 19 August, 1999 the source was known to be in a particlular region of the color-color diagram based on results in the published literature.

As shown in Table 2 the average spectra comprise a number of continuum and atomic transition components: (a) A low temperature disk blackbody of innermost temperature $T_{in} \simeq 1$ keV. (b) A blackbody component of $T_{bb} \sim 2$ keV attributed to the boundary layer. (c) A power law with index $\Gamma \simeq 2$, presumably the result of the Comptonization of the disk or boundary layer photons by the accretion disk corona. (d) An Fe line feature at $E_c \sim 6.6$ keV and, (e) An Fe line edge at $E_{edge} \sim 9.5$ keV. In figs 2a,b. we present the overall spectrum as the decomposition of these three components for two epochs when the source was in its island (09 Feb. 2001) and upper banana (21 Sep. 1997) states. The disk blackbody component is not required in the spectrum of the island state (IS) of Feb 09, 2001 but it is necessary to fit the lower banana (LB) and upper banana (UB) branch spectra. The blackbody temperature T_{bb} appears to increase as the source moves from the IS to the UB while its normalization traces the overall increase in the source counts along the above sequence. The progression from the IS to the LB and UB states is also accompanied by an increase of the power law normalization and its index Γ. The latter is usually interpreted as a steepening of the Comptonization spectrum due to the cooling of the Comptonizing electrons by the increased soft (blackbody) photon flux.

We have also found that the source variability properties change markedly with

the spectral state. First, as shown in Table 1 the break and QPO frequencies increase monotonically as the source flux and power law index Γ increase. In Fig 3 we present the PSD of the source in three different spectral states. The island state exhibits the highest RMS variability at all frequency bands, its νP_ν spectrum exhibiting a maximum at the limit of the searched frequencies (~ 500 Hz). In the lower banana state the νP_ν spectrum rises from the low frequencies to a plateau (i.e. $\nu P_\nu \propto \nu^0$ at $\nu \sim 20$ Hz) and the RMS variability is lower at all frequencies than that of the island state. Finally, in the upper banana state the shape remains qualitatively similar to that of the LB but with greatly reduced amplitude and the additional appearance of excess power at frequencies lower than 0.3 Hz. We believe that this sequence in the timing properties is suggestive of the progressive influence of the effects of radiation pressure in the accretion process (negligible in the IS but progressively important towards the UB state). It is reasonable to consider the possibility that the radiation feedback on the flow could damp the short scale variability by the diffusion of photons through the accreting plasma; inundating the system with soft photons that could conceivably also reduce the overall variability amplitude (Kazanas & Hua 1999).

4. Fourier Resolved Spectral Analysis

In this section we present the results of our Fourier resovled spectral analysis for each state and compare the resulting best-fit parameters to those of the previous section (i.e, those obtained from the average energy spectra). As before, the XSPEC package was used for the model fitting. In all cases we added an absorption component which we fixed at 3×10^{22} cm^{-2} (e.g. Narita, Grindlay & Barret, 1999). A uniform systematic error of 1% was added quadratically to the statistical error of all Fourier spectra in each energy channel. Errors quoted for the best-fit values correspond to the 90% confidence limit for one interesting parameter.

The virtue of the frequency-resolved spectra is that they receive significant contribution only from the spectral components that are variable on the time scales sampled; the FRS do not represent photon rates but rather variability amplitudes at a given energy. Therefore, through Fourier-resolved spectroscopy we can investigate whether different spectral components in the overall spectrum of the source (e.g. blackbody, Comptonization, iron line) are variable and at which frequency. In general, the interpretation of the FRS is not unique (see Papadakis et al. 2005, Reig et al. 2006 for some insights). For spectral features that result from the reprocessing of higher energy ($E \geq 7$ keV) continuum, such as the iron Fe Kα line and the Compton reflection "hump", one plausible interpretation of the Fourier-resolved analysis is that the light crossing delay R/c (where R is the size of the reprocessing region) filters out variability of these features on frequencies higher than $\sim c/R$. We would note that while this interpretation may be the most straightforward one,

other interpretations, such as scenarios involving screening geometries are also possible e.g. (Revnivtsev et al. (1999)).

In the following subsections we describe the results of our analysis for each of the spectral states of the source. In addition to the four sets of data mentioned above, we analyzed data for three additional epochs for which the spectral state of the source was previously documented. Our objective is to compare the results obtained above with the traditional designations of island and banana states in order to characterize the spectral and timing properties of each state. We searched in the literature for observations for which 4U 1728–34 was clearly identified as being in one of the characteristic atoll states. 4U 1728–34 was in the island state on June 7, 2001 (Migliari et al. 2003), upper banana state on August 19, 1999 (Piraino et al 2000) and lower banana state on February 18, 1996 (di Salvo et al. 2001).

4.1. The Island State

The source was in the island state on Feb. 09, 2001, and, as noted by Migliari et al. (2003) 4U 1728–34 also appeared to be in the island state during the June 7, 2001 observations. We obtained the 64-channel, 1-ms data sets from those observations and formed the FRS as described in §3. We found that a single-temperature blackbody model led to fits which were unacceptable, particularly at our low-frequency band. In particular, residuals at the low- and high-energy channels were evident. Improved fits were provided with an additive combination of the blackbody plus a powerlaw. The powerlaw required is rather flat $\Gamma \simeq 0.5$, but is is poorly constrained, particulary in the Feb. 09, 2001 observation. The reason is that in those model fits the blackbody is the predominant component except in the (several) highest energy energy bins.

The blackbody component in these cases is characterized at each frequency band by a temperature of about $kT = 1.0 - 1.7$ keV without an obvious trend. The spectral decomposition parameters for the island-state FRS are given in Tables 3 and 4. As summarized there and shown in fig. 5, the Feb. 9, 2001 FRS, for example, can be fitted well by a blackbody plus powerlaw spectrum with temperature $kT \sim 1.5 - 1.7$ keV, similar in magnitude to the temperature $T_{\rm bb}$ of the conventional spectra attributed to emission by the boundary layer. The Power Law (energy) spectral indices are quite hard ($\simeq 0.6$) although they are marginally constrained. The same spectra can actually be fit by a simple power law absorbed at low energies, without the presence of a black body component. A summary of such fits is given in Table 3, for an absorbing column of $N_H = 3 \times 10^{22}$ cm^{-2}. Also see 5. The fits exhibit no particular trend with Fourier frequency.

We also tested several other simple models. A powerlaw model with low-energy

cutoff was unable to constrain the inflection energy value and broken powerlaw fits led to unacceptable results.

There seems to be a general trend in the island state FRS towards hard or even positively sloped spectral-energy distributions, i.e. a trend variablity to increase with energy. This is particularly notable for example in the low-frequency spectra for both island state epochs (Tables 3 and 4), and it is consistent with the RMS variability versus energy analysis of Revnivtsev et al. (2000). This is reminiscent of Blazar variability.

While none of the FRS results require an iron line - upper limits on its equivalent width range from a few hundred to a thousand eV - it is clearly seen in the conventional spectra for 3 of the 4 epochs denoted in Table 2; specifically the EW determination indicates a $\sim 10\sigma$ significance in several cases. The FRS are harder than the averaged spectra, indicating again that the hard emission may be the predominant component of the source variability.

Finally, we note that although the island-state count rate was lower by about a factor of 10 than the banana-state cases, the rms variability in the island state is significantly higher. Thus, the statistics of the island-state FRS are comparable or superior to those of some banana state epochs.

4.2. The Lower Banana state

On Jan. 25, 1999 as well as on Feb. 18, 1996 (also see di Salvo et al. 2001) the source intensity along with the PDS break frequency at about 16 Hz, indicated that 4U 1728–34 was in the the lower banana state. A single blackbody model provides acceptable fits for all three of our frequency ranges (our fit results are summarized in Table 5). Its temperature is consistent with that of the time averaged spectra, indicating that it is the boundary layer component which is responsible for the source variability. The absence of the power law and Fe line components that are present in the time averaged spectral fits, suggests that these components are not variable on the time scales examined. The normalization of this component is comparable in the low and high frequencies and slightly lower at the mid-frequency range, indicating that all frequencies contribute roughly equally to the variations of this component.

The single blackbody fit to the FRS for various banana spectral states, and for the three frequency bands have characteristic temperatures that span the nominal kT$\simeq 2 - 3$ keV range. However, no unambiguous trends with temperature versus frequency are seen.

4.3.   The Upper Banana State

The source was found to be in the upper banana state on Sept. 26 and Sept. 21 1996, as determined by the value of the PSD break frequency ν_b. We also obtained data for the upper banana state noted during August 19, 1999 by (Piraino et al. 2000). In this case, we found that the RMS variations above $\sim$8 Hz (high-frequency) were apparently small as we were unable to obtain useful signal-to-noise for any of our FRS bands for these data. The overall count rate on the other hand was high, ~ 10 times that for the island state. As discussed above a single blackbody provides a good fit to the FRS without the need for additional components at any of the frequency bands. The amplitude of this component appears to increase with decreasing frequency in the 1996 observations while remained the same during the 1999 one, thus indicating that this attribute of the spectra is not characteristic of the particular state.

5.   Discussion

We have investigated the spectro-temporal characteristics of the atoll X-ray binary 4U 1728–34. To this end we have produced the energy and power spectra of the source in its different spectral states, i.e. island (IS), lower banana (LB) and upper banana (UB) and also the Fourier-resolved spectra (FRS) of each state for three different frequency bands.

Fits of the time average spectra of the source require a combination of a blackbody (to model the boundary layer emission), a multicolor blackbody (to model emission by the accretion disk), a power law (to model coronal emission), an Fe line and a low-energy galactic-absorption column of $N_H = 3 \times 10^{22}$ cm^{-2}. The results for the conventional spectra are given in Table 2. As the source crosses from the island to the lower and upper banana states the source spectra change significantly (see Fig. 1). Our spectral decomposition indicates for this sequence the component exhibiting the largest parameter range is the multi-color disk. While its presence is not required in the island state, it is necessary for acceptable fits in the other states with approximately constant temperature and highly variable normalization. Unfortunately, the RXTE spectra do not cover the energy regime $E < 2$ keV, necessary for the more accurate determination of this component. Also variable is the index Γ of the power law component; the increase of Γ with the total flux of the source is generally attributed to the decrease in the temperature of the Comptonizing medium by the increase of soft thermal photon flux and the resulting Compton cooling effects. The temperature of the blackbody component exhibits an increase between the island and the banana states (referring to the blackbody plus powelaw fits to the island state), but it appears to remain constant once the banana states are reached. This suggests a behavior different from that of the Z-sources. Gilfanov et al. (2003) find from their FRS analysis

that the temperature of this component remains constant, suggesting that the sources' boundary layer is radiation pressure dominated. Following the same argument, the increase of the thermal component temperature with increasing source flux leads to the conclusion that in the atoll sources the boundary layer is not radiation dominated in the island state, while it appears to become so in the banana states. Finally, the EW of the Fe line appeared to remain constant to within statistics throughout the source's spectral sequence.

The variability properties of the source, as manifest by the source power-density spectra, change significantly with its spectral state: The overall RMS fluctuations across all frequencies decrease with increasing source flux; in addition the PDS shape changes as the source moves from the island to its banana states (see Fig. 3). Finally, in the general case, the frequency of features in the PDS such as breaks and QPOs increase along the island to upper banana sequence. We suggest that the decrease in variability is due to the effects of radiation pressure on the accretion flow, which through diffusion damps the high frequency components and the overall amplitude.

We have elaborated further on the study of the spectro-temporal properties of the source by producing its Fourier-resolved spectra at three frequency bands for each of the source's spectral states, namely $0.008 - 0.8$ Hz, $0.8 - 8$ Hz and $8 - 64$ Hz. While interesting features in the Fourier domain are known to occur at higher frequencies (i.e. kHz QPO) our data did not allow the application of this technique to these frequencies with any significance. The source state was determined either from prior analysis gleaned from the published literature or was defined by the spectral hardness–break frequency correlation. In the latter cases, we mostly relied on the measurements and analysis of (Titarchuk & Shaposhnikov 2005), but in several instances we measured these quantities ourselves. Several notable trends are gleaned from our analysis and are identified below.

The results of our FRS analysis can be summarized as follows:

(i) The iron line at $\sim$6.6 keV, distinctly present in the conventional spectra ($\simeq 10\sigma$ for the banana state cases), is not apparent in any of our frequency-resolved spectra. For example, when we fix the line energy at 6.6 keV and the width to 0.6 keV, we derive only upper limits on the equivalent widths (values ranged from about 50 to 600 ev). This suggests that, at leaset within the limitations of our measurements, there may be no significant Fe line variability on time scales between $10^{-2} - 10^2$ s. This is in agreement with the lack of correlation between the Fe Kα equivalent width and QPO frequencies reported by (Titarchuk & Shaposhnikov 2005). These authors concluded that the size of the Fe Kα emitting region is not of the same order as that of the X-ray continuum emission, the former possibly being orders of magnitude larger than the latter. On the other hand, a different view has been promoted by Miniutti et al. (2003) with respect to the Fe line variability in AGN. In as much as the geometry and physics of Fe line production in these very diverse objects is similar, such an interpretation should also be considered.

– 13 –

(ii) No disk component is present in the FRS, indicating as in the case of the iron line, that the accretion disk emission is significantly less variable at the frequencies sampled by our study, i.e. 0.08-64 Hz. This result agrees with those found in other neutron-star (Revnivtsev & Gilfanov 2006) and black-hole (Reig et al. 2006) binaries.

(iii) We have examined five data sets corresponding to the banana state spectral/temporal configuration. Our FRS reveal that the temperature of the thermal spectral component is consistent with being constant across frequencies and states. Unfortunately, this statement cannot be made with high degree of confidence for the UB states as the decrease in the variability amplitude makes the determination of the Fourier resolved parameters of the spectra difficult.

(iv) Two observations corresponding to the island state reveal evidence for a spectral hardening at the lowest frequencies examined. The island state are generally harder than the corresponding frequency averaged spectra. Single blackbody model fits to the island state FRS, were unsatisfactory, with a significant high-energy residual appearing, particularly for our lowest frequency interval. The addition of a hard powerlaw component leads to improved fits to the data, although the slope is poorly constrained. We have also tried an alternative models, the most satisfactory of which was a single power law with a low energy neutral absorpion by a column of $N_H = 3 \times 10^{22}$ cm^{-2}. It was found that this presents an good fit to the data with the corresponding parameters as given in Table 3. In general, the FRS are notably harder than the conventional spectra for the island state, indicating a substantial contribution of the high-energy emission to the source variablity, at least for this spectral state, a situation not unlike that found in other studies as previously referenced.

(v) The results of our FRS analysis are in general agreement with those of Gilfanov et al. (2003) of Z-sources, in that the FRS spectra are dominated by a single blackbody component of constant temperature when $\dot{M} \sim 0.1 - 1 \ \dot{M}_{\mathrm{Edd}}$, that is, for Z sources and atoll sources in the banana state. This is attributed to emission by the boundary layer which in addition is radiation pressure dominated hence the independence of the temperature on the source flux (the local flux is always that of Eddington). The temperature of this component is consistent with that of the blackbody component in the time average spectra.

(vi) Finally, we have extended the study of the Fourier-resolved spectra of neutron-star low-mass X-ray binaries to the lower luminosity end. Previous studies had concentrated on higher luminosity states of these objects, i.e., Z-sources or atoll sources in their soft/high spectral state (Gilfanov et al. 2003; Gilfanov & Revnivtsev 2005; Revnivtsev & Gilfanov 2006). The X-ray luminosity in the 2–16 keV range of 4U 1728–34 in the island state, assuming a distance of 4.3 kpc (Foster etal. 1986) is $\sim 3 \times 10^{36}$ erg s^{-1}, i.e. $\sim 10^{-2} L_{\mathrm{Edd}}$, about one order of magnitude lower than previous studies. We found that the temperature of the blackbody component of the conventional spectrum of the island state is significantly

lower than that of the corresponding FRS when the powerlaw plus blackbody model is applied. The most straightforward interpretation of this fact is that the conventional island-state spectrum includes contribution from a component of lower temperature and little variability.

Future applicaton of Fourier-Resolved spectroscopy to low-mass X-ray binaries, incorporating both larger data sets and additional objects of the representative subclasses offers the posiblity for furher insight into each of these issues.

Acknowledgements

REFERENCES

di Salvo, T., Méndez, M., van der Klis, M., Ford, E., Robba, N.R. 2001, ApJ, 546, 1107

Ford, E., & van der Klis, M., 1998, ApJ, 506, L39

Foster, A. J., Fabian, A. C., Ross, R. R. 1986, MNRAS, 221, 409

Gilfanov, M., Churazov, E. & Revnivtsev, M. 2000, MNRAS, 316, 923

Gilfanov, M., Revnivtsev, M., & Molkov, S., A&A, 410, 217

Gilfanov, M., & Revnivtsev, M. 2005, Astr, Nachr., 326, 812

Kazanas, D. & Hua, X.-M., 1999, ApJ, , 519, 750

Mendez, M., & van der Klis, M., 1999, ApJ, 517, L51.

Migliari et al., 2003, MNRAS, 342, L67

Narita, T., Grindlay, J.E., and Barret, D., bull AAS, 31, 904

Papadakis, I. E., Kazanas, D., & Akylas, A. 2005, ApJ, 631, 727

Papadakis, I.E., Ioannou, Z., & Kazanas, D., 2006, ASNA, 327, 1047

Piraino, S., Santangelo, A., & Kaaret, P., 2000, A&A, 360, L35

Reig, P., Papadakis, I.E., Shrader, C.R., & Kazanas, D., 2006, ApJ, 644, 424

Revnivtsev, M., Gilfanov, M., & Churazov, E. 1999, A&A, 347, L23

Revnivtsev, Mikhail G., Borozdin, Konstantin N., Priedhorsky, William C.,& Vikhlinin, Alexey 2000, Ap.J., 230, 955

Revnivtsev, M., Gilfanov, M., & Churazov, E. 2001, A&A, 380, 502

Revnivtsev, M. G., Gilfanov, M. R. 2006, A&A, 453, 253

Sobolewska, M.A., & Zycki, P.T., 2006, MNRAS, 370, 405

Titarchuk, L. & Shaposhnikov, N. 2005, ApJ, 626, 298

van der Klis, M., 2000, ARA&A, 38, 717

van der Klis, M., 2006, in "In: Compact stellar X-ray sources", Ed. by W. Lewin & M. van der Klis. Cambridge Astrophysics Series, No. 39. Cambridge University Press.

Vignarca, F., Migliari, S., Belloni, T., Psaltis, D., van der Klis, M. 2003, A&A, 397, 729

Wijnands, R., 2001, AdSpR, 28, 469

Zycki, P., 2003, ASPC, 290, 135

Table 1: Log of the observations

Epoch	Γ	ν_b (Hz)	Source state	2-16 keV flux (c/s)*	Exposure time(ks)
Feb 9, 2001	1.40	0.75	IS+	640	4.40
Jan 25, 1999	2.07	12.54	LB+	1824	11.3
Sep 26, 1997	2.88	24.2	UB+	1659	12.8
Sep 21, 1997	5.54	41.55	UB+	1953	13.5
Jun 7, 2001	1.46	0.9	IS	445	6.91
Feb 18, 1996	2.41	12.21	LB	1380	3.33
Aug 19, 1999	3.35	24.1	UB	2600	2.05

*For 5 PCU

+Inferred from PDS

Table 2: Conventional Spectral Analysis Results

Observation	Feb 9, 2001	Jan 25, 1999	Sep 26, 1997	Sep 21, 1997
Flux[1] (erg s^{-1} cm^{-2})	1.4	4.1	3.8	4.6
DISKBB				
T_{in} (keV)	–	$1.7^{+1.1}_{-0.5}$	1.06±0.03	1.4±0.1
norm	–	5^{+10}_{-4}	110±15	45^{+20}_{-10}
BBODY				
kT_{bb} (keV)	1.27±0.05	2.3±0.4	2.1±0.1	2.2±0.1
norm ($\times 10^{-2}$)	0.34±0.08	$1.3^{+0.5}_{-0.1}$	2.8±0.1	3.3±0.3
POWER LAW				
Γ	1.75±0.04	2.03±0.08	2.1±0.2	$2.3^{+0.2}_{-1.4}$
norm	0.28±0.04	1.0±0.2	0.4±0.2	0.42±0.05
GAUSS				
E_c (keV)	6.6±0.2	6.6±0.2	6.5±0.3	6.6±0.3
σ (keV)	0.5±0.4	0.6±0.2	0.8±0.3	0.7±0.3
EW (eV)	100±60	150±15	180±20	140±15
EDGE				
E_{edge} (keV)	–	9.5±0.5	9.6±0.6	9.9±0.6
τ	–	0.04±0.02	0.04±0.03	0.04±0.03

All fits include a fixed absorption component with $N_{\mathrm{H}} = 3 \times 10^{22}$ cm^{-2}

[1]: $\times 10^{-9}$ in the energy range 2–16 keV

Table 3: Results of the spectral fits (single power law) to the Fourier-resolved spectra spectra of the island state. The fits include an absorption compoonent with fixed $N_H = 3 \times 10^{22}$ cm^{-2}.

Observation	09/02/01	07/06/2001
0.008–0.8 Hz		
Γ	1.7±0.1	1.8±0.2
norm ($\times 10^{-2}$)	2.0±0.3	0.9±0.4
0.8–8 Hz		
Γ	1.7±0.1	1.7±0.2
norm ($\times 10^{-2}$)	3.4±0.6	1.6±0.5
8–64 Hz		
Γ	1.6±0.3	1.4±0.6
norm ($\times 10^{-2}$)	3.0±1.5	1.0±0.8
χ^2/dof	1.5/52	0.91/46

Table 4: Results of the spectral fits (blackbody plus power law) to the Fourier-resolved spectra spectra of the island state

Observation	09/02/01	07/06/2001
0.008–0.8 Hz		
$kT_{\rm bb}$ (keV)	1.7±0.1	1.0±0.3
norm ($\times 10^{-3}$)	0.7±0.1	0.19±0.04
Γ	0.6±0.3	0.4±0.7
norm ($\times 10^{-3}$)	0.55±0.06	0.35±0.07
0.8–8 Hz		
$kT_{\rm bb}$ (keV)	1.5±0.1	1.7±0.3
norm ($\times 10^{-3}$)	1.0±0.1	0.5±0.1
Γ	0.6^f	0.4^f
norm ($\times 10^{-3}$)	1.4±0.1	0.32±0.06
8–64 Hz		
$kT_{\rm bb}$ (keV)	1.7±0.6	$1.0^{+2.0}_{-0.5}$
norm ($\times 10^{-3}$)	$0.9^{+0.9}_{-0.4}$	0.9±0.3
Γ	0.6^f	0.4^f
norm ($\times 10^{-3}$)	1.6±0.4	0.8±0.2
χ^2/dof	0.90/51	0.73/43
F-test prob.*($\times 10^{-2}$)	7×10^{-8}	7×10^{-6}

^{f}: fixed parameter

*: probability that the addition of the power-law component occurs by chance

Table 5: Results of the spectral fits (blackbody) to the Fourier resolved spectra spectra

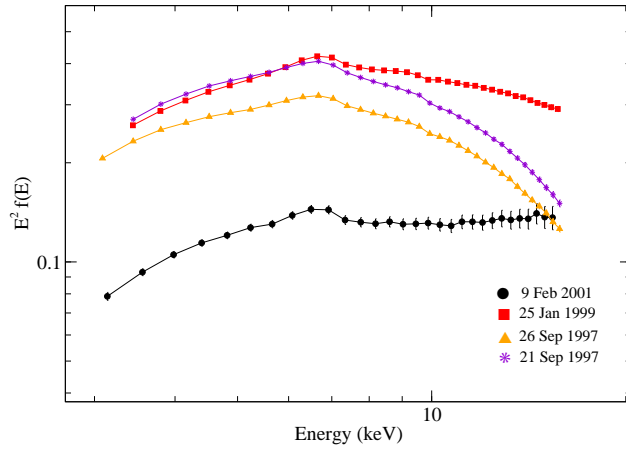| Observation	Feb 18, 1996	Jan 25, 1999	Sep 26, 1997	Sep 21, 1997	August 19, 1999
0.008–0.8 Hz					
kT_{bb} (keV)	2.7±0.4	2.27±0.04	2.27±0.04	2.14±0.05	2.4±0.2
norm ($\times 10^{-3}$)	1.0±0.1	4.8±0.1	5.0±0.1	3.7±0.1	1.8±0.1
0.8–8 Hz					
kT_{bb} (keV)	2.10±0.08	2.02±0.05	2.3±0.2	2.1±0.4	2.5±0.5
norm ($\times 10^{-3}$)	2.6±0.1	3.07±0.07	1.5±0.2	1.4±0.3	2.2±0.4
8–64 Hz					
kT_{bb} (keV)	2.18±0.09	2.15±0.07	2.2±0.4	2.2±0.3	2.8±0.6
norm ($\times 10^{-3}$)	4.2±0.2	4.6±0.1	2.2±0.3	2.5±0.3	4.0±0.8
χ^2/dof	0.95/37	1.80/64	1.05/53	0.94/55	0.95/39

Fig. 1.— Results of our (conventional) spectral analysis for the various epochs and corresponding spectral state configurations. The spectra are satisfactorily fitted with an absorbed blackbody plus multi-color accretion disk components at low energies and a power-law component at higher energies. An Fe line plus edge were also required (see Table 2).
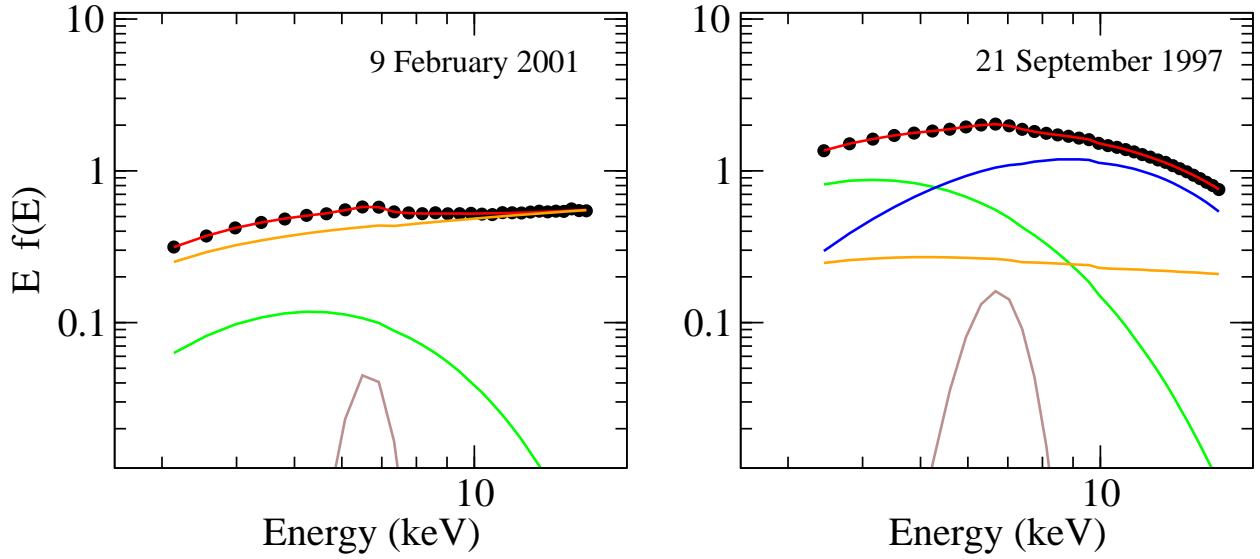
Fig. 2.— Spectral decomposition of the average source spectra for the island (09 February 2001) and upper banana (21 September 1997) states. The model components are described in the text and in Table 2, and are plotted in νf_ν space. Specifically, for Feb. 9 2001 a blackbody component (green), powerlaw (brown) and a gaussian line (purple) are depicted; for Sep. 21 1997 one can also see the blackbody component (blue), the multi-color disk (green), the powerlaw (brown) and the line (purple). As the source flux increases so does the blackbody temperature, the index of the power law and the Fe line flux.
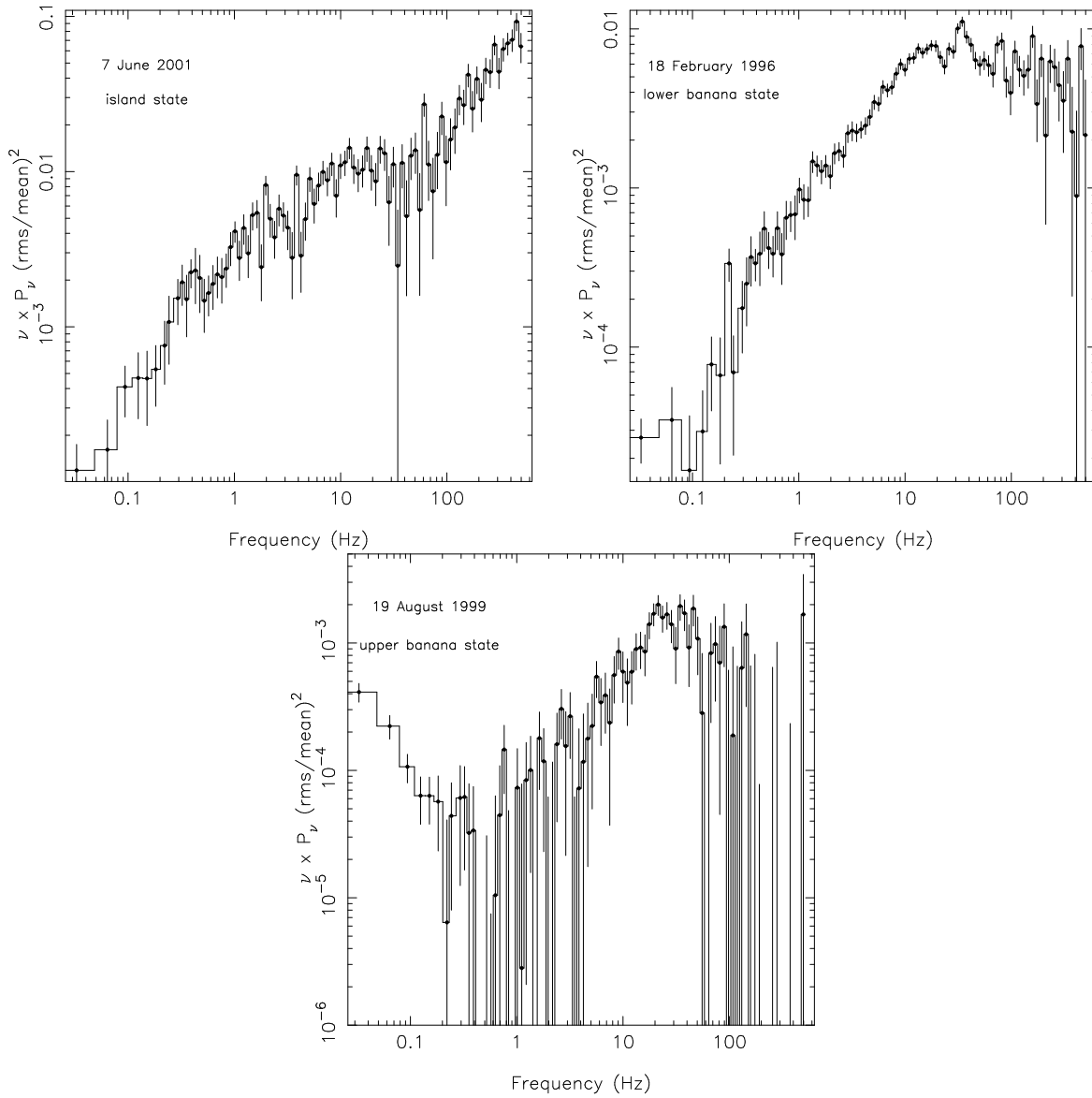
Fig. 3.— Power spectral density for the representative states of 4U 1728–34: island state, 7 June 2001 (upper left), lower banana state, 18 February 1996 (upper right) and upper banana, 19 August 1999 (lower).
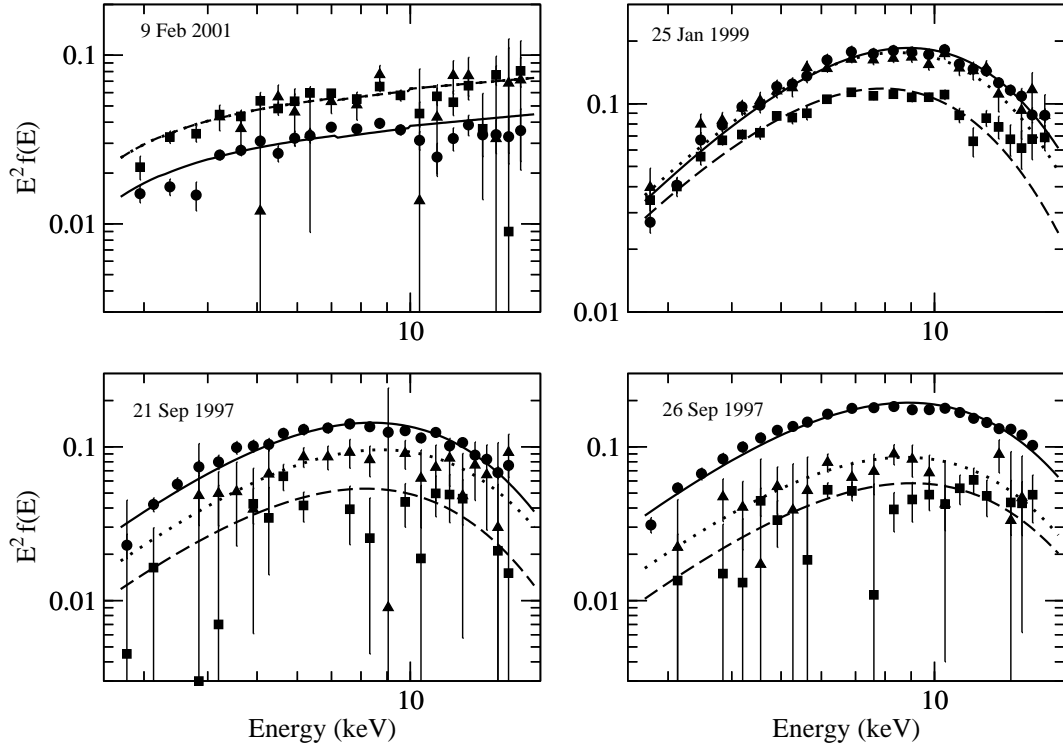
Fig. 4.— Fourier resolved spectra and their corresponding spectral-model fits for the days annotated in the figure. The different frequency bands are as follows: circles $0.008 - 0.8$ Hz; squares $0.8 - 8$ Hz; triangles $8 - 64$ Hz. The solid, dashed, and dotted curves are the respective model fits plotted in νf_ν space.
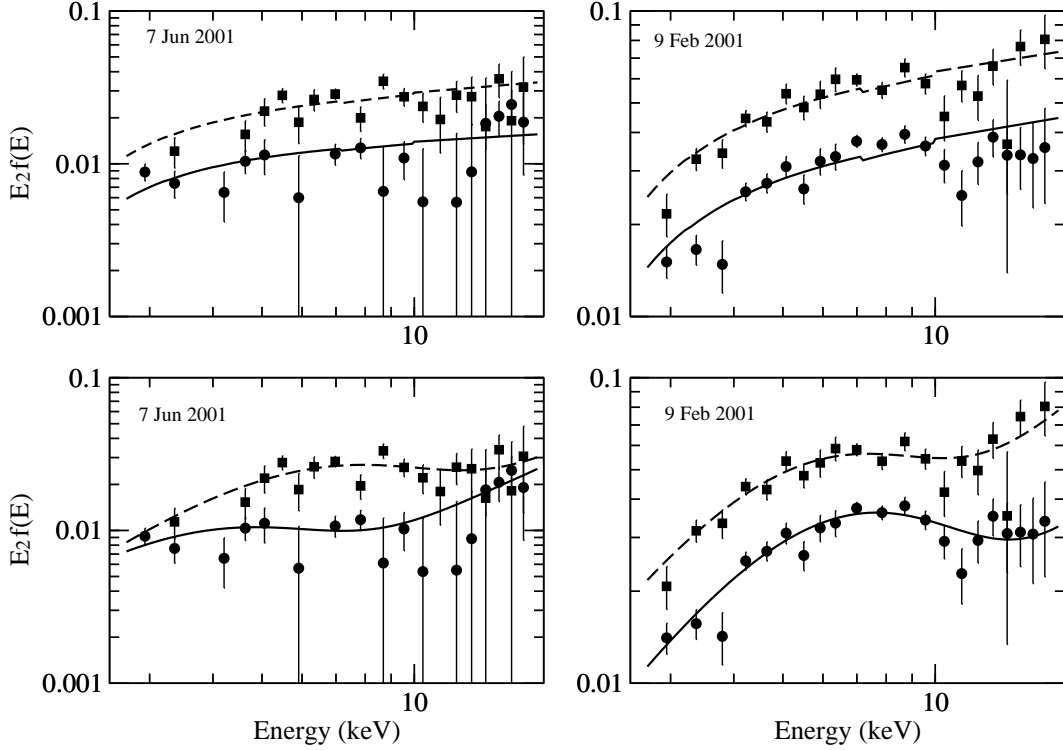
Fig. 5.— The upper figures show the low- and medium-frequency spectra for (a) the June 7, 2001 and (b) February 9, 2001 island state observations fitted to an absorbed powerlaw model (refer to 3 for the parameter values). The solid curves are the model in νf_ν space with the FRS spectral data points overlayed. The lower figures show the spectral decomposition of the same two data sets with an additive blackbody plus powerlaw model.